

We are IntechOpen, the world's leading publisher of Open Access books Built by scientists, for scientists

6,900

Open access books available

185,000

International authors and editors

200M

Downloads

Our authors are among the

154

Countries delivered to

TOP 1%

most cited scientists

12.2%

Contributors from top 500 universities



WEB OF SCIENCE™

Selection of our books indexed in the Book Citation Index
in Web of Science™ Core Collection (BKCI)

Interested in publishing with us?
Contact book.department@intechopen.com

Numbers displayed above are based on latest data collected.
For more information visit www.intechopen.com



Geothermal Explorations on the Slate Formation of Taiwan

Sheng-Rong Song and Yi-Chia Lu

Abstract

Currently, over 90% operated geothermal power plants are distributed in the volcanic- or magmatic intrusion-related geological systems. Only a few cases are done in metamorphic terranes, especially on the slate formation. Taiwan is located at the ring of fire and is famous for the young orogenic belt, which has wide distributions of rapid uplifting terranes with few active volcanoes. The metamorphic rocks, for example, schist and slate formations with high geothermal gradients, are occurring in the major mountain range. This chapter introduces the techniques or methods we used for geothermal exploration in the slate formation of the Chingshui geothermal field of Taiwan, where a 3-MW pilot geothermal power plant had been installed in 1983 and operated for 12 years.

Keywords: Chingshui geothermal field, Taiwan, slate formation, calcite veins, clumped isotope

1. Introduction

Energy is the essential lifeblood of today's national economy. Diversification of energy sources is reasonable and important in establishing policy for all countries in the world. Among various energy sources, geothermal energy offers a naturally free resource and less dependence on fossil fuels. Taiwan is a country in which the energy is very scant, and almost over 99% consumed ones, most of the fossil fuels, are imports from outside of this country [1]. Taipower, the only commercialized power company in Taiwan, has installed capacity of 40.79 GWe, which produces the gross electricity of about 219.2 billion kWh [2]. They are produced by fossil fuels including oils, coals, and natural gases, nuclear power, hydropower and renewable energy, etc. Among them, the majority is the fossil fuels (72.78%) followed by nuclear power (18.61%), while the renewable energy only occupies 2.86%. There are four nuclear power plants in Taiwan, namely, No. 1, No. 2, No. 3, and No. 4, three of which are in operation and the fourth is under construction, but the latter is sealed now due to it being considered as non-safe after the 2011 Fukushima nuclear disaster in Japan and because of the nuclear-free policy. Moreover, those three operating ones are old, more than 30 years old, and will be decommissioned from 2018 to 2025. The electricity will be less than 18.61%, about 40.79 billion kWh per year, and there is a need to find alternatives for them in the next 10 years in Taiwan. It, thus, provides an opportunity for developing geothermal energy.

Taiwan is located at the ring of fire and is famous for the young orogenic belt (**Figure 1**), which has wide distributions of rapid uplifting terranes with few active volcanoes [3, 4]. Three geothermal play types have been distinguished in

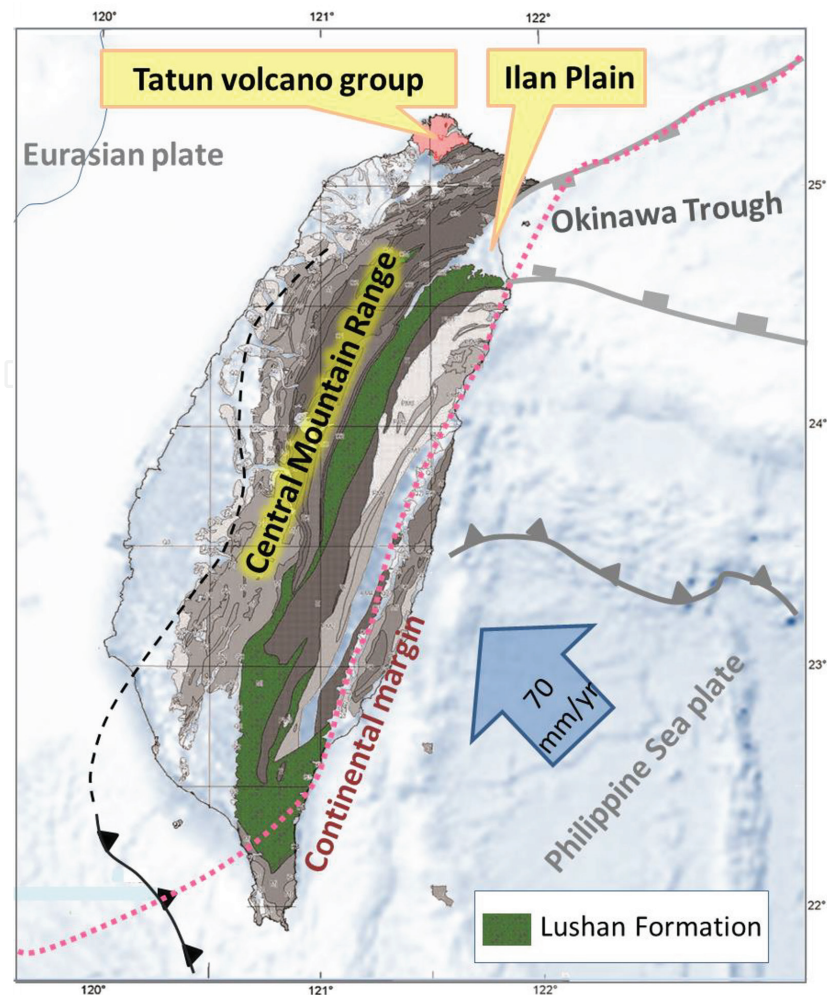


Figure 1.
The tectonic framework of Taiwan.

terms of geological controls [5, 6]. They are the magmatic-volcanic field type, the extensional domain type, and the orogenic belt/foreland basin type, which are correlated to the Tatun volcano group, the Ilan Plain, and the Central Mountain Range, respectively (**Figure 1**). Lot of geothermal explorations have been done in this island since the 1960s, and two pilot geothermal power plants had been built up in slate formation in northeast Taiwan [7]. In 2005, the Bureau of Energy of Taiwan revisited the slate formation for geothermal exploration and developed a plan for future power generation in the Chingshui geothermal field. The Ministry of Science and Technology (MOST) (formerly known as the National Science Council, NSC) of Taiwan initiated and promoted the geothermal explorations and developments as a major national energy project (NEP I and II) since 2008. The works include more precise geological, geochemical, and geophysical surveys with drillings [8]. Currently, over 90% of the on-working geothermal power plants are operated in the volcanic- or magmatic intrusion-related systems [9]. There are only few cases of metamorphic terrane, especially on the slate formation. The aims, thus, of this article are to introduce the techniques or methods we used for geothermal exploration in the slate formation of the Chingshui geothermal field of Taiwan.

2. Geological background

Taiwan belongs to the ring of fire and is famous for active orogeny (**Figure 1**). Presently, the Philippine Sea plate is moving toward WNW at about 70 mm/yr. [10],

and it is believed that the mountain-building process is still ongoing [11, 12]. A dominant collision zone frequently inducing folding and fault thrusting in the area may exist in central Taiwan and cause rapid uplifting rate being 6 mm per year [13]. Tectonically, the Philippine Sea plate is riding up over the continental shelf of the South China Sea in southern Taiwan. Moreover, an oceanic part of the Eurasian plate is subducting beneath the Philippine Sea plate along the Manila trench, which results in the bulldozing of shelf sediments both upward and westward. This island of Taiwan has been created in the last 5 million years [3, 14, 15], and rapid crystal movements and widely distributed active structures make up the geological characteristics of this young tectonic entity [16–19]. In the north, the Philippine Sea plate subducts underneath the Eurasian plate, leading to the formation of Ryukyu arc (**Figure 1**). The Okinawa Trough is a back-arc basin, which extends from southwest Kyushu Island (Japan) to the Ilan Plain, which is the southwest-most tip of it. Three stages of opening have been identified since 15 Ma, and the latest phase of extension occurred in the southwestern part of the Okinawa Trough, which is characterized by normal faults with vertical offsets since the late Pleistocene [20–22]. The age of the normal stress affecting the Ilan Plain may be in the latest Pleistocene; based on the thermoluminescence (TL), age of 7.0 ± 0.7 ka obtained from a siltstone xenolith was found at Kueishantao, an offshore volcanic island 10 km away from the coast of Ilan Plain [23]. Several active volcanoes have been identified in inland and offshore of this island, and high uplift mountain range occurs in the eastern and central parts of Taiwan. Those tectonic settings provide a very good environment rich in geothermal energy.

The slate formation, named the Lushan Formation, is widely distributed in the Backbone Range belt of Central Range, Taiwan (**Figure 1**). It is composed of argillite and slate of early to middle Miocene. The type locality of this formation is located in the Lushan area, east of Wushe in Nantou County. Miocene foraminifers were found in slates and marly nodules in this formation, which extend for an east–west width of at least 14 km on the western slope of Central Range [24, 25]. The Lushan Formation consists largely of black to dark-gray argillite, slate, and phyllite with occasional interlayer of gray sandstones. The estimated thickness is several thousand meters. This formation is exposed in north Taiwan at the mouth of the Lanyang River in the Ilan County and extends southward along the crest zone of the Central Range through Hohuashan, Nengkaoshan, to Hsiukuluanshan for a length of approximately 150 km and a width of several to 10 or more kilometers [26]. South of the Yushan Mountain, the Lushan Formation occurred east of the Laonong River southward to the eastern mountains of the Pingtung valley down to the Hengchun Peninsula. It also crops out in southeastern Taiwan in the area of Chihpen and Tawu [26].

3. Geology of Chingshui geothermal field

The Chingshui geothermal field is located in the valley of Chingshui stream, southwest of Ilan Plain, northeast Taiwan (**Figure 2**). The rock hosting the geothermal field is the Miocene Lushan Formation, consisting dominantly of argillite/slate with intercalated thin meta-sandstones [27, 28]. Several hot springs with minor hydrothermal alterations are the important thermal manifestations, which they crop out along the riverbed and rock cliffs in this area (**Figure 3A**). Temperatures and TDS of them range from 34°C to over 95°C and from 896 to 1500 ppm, respectively. Hydrothermal minerals include calcite, aragonite, dolomite, strontianite, amorphous silica, burbankite, kaolinite, sulfur, jarosite, tschermigite, and gypsum.

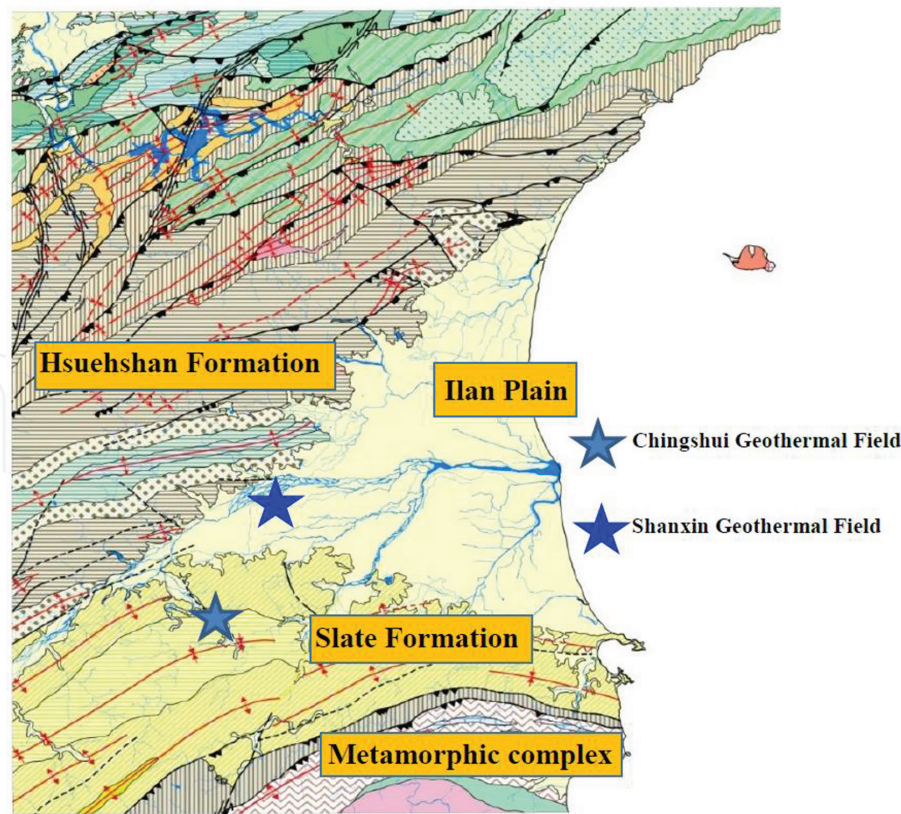


Figure 2.
The Chingshui geothermal field is located in the valley of Chingshui River, which is in the southwestern Ilan Plain.

These field investigations and subsurface geological reports indicate that the Lushan Formation in this area is composed predominantly of dark-gray and black slates with thinly layered meta-sandstones, which can be divided into three members. They are the Jentse member, the Chingshuihu member, and the Kulu member. The upper Jentse member consisting of mainly light meta-sandstone intercalated in dark-gray slates, while the lower Chingshuihu and Kulu members consist mostly of slates [27, 28]. Two regional folds according to the vergence from minor folds in the thin-bedded sandstone have been identified in the Chingshui geothermal field [29]. The synclinorium axis is located within the Jentse member across the upstream region of the Chingshui River. The anticlinorium axis is located across the downstream region of Chingshui in the Chingshuihu member. Both fold axes were offset by the Chingshui Fault.

Several faults, including the Xiaonanao and Chingshui faults and a few small unnamed ones, cut through rock bodies in Chingshui area (**Figure 3A**). The Xiaonanao Fault is a thrust fault with wide damage zones that are rich in quartz veins on the outcrops along the Chilukeng River (**Figure 4**). The fault stretches to the east where an upside-down sequence of strata appears at the Shimen River [28]. The Chingshui Fault is a south–north strike-slip one inferred from geophysical data [30, 31]. The geothermal field, therefore, cropped out follows the surface trace of the suspected Chingshui Fault along the Chingshui Valley [27, 30, 32] (**Figure 3A**). Those normal faults, therefore, in the area were formed during the Pengli orogeny in the late Pliocene [33]. However, some outcrops of other faults cannot be found on the surface after heavy weathering and erosion in the area.

There are many parallel normal faults with strike-slip component gouges (inferred by slickenside direction) approximately 200 m long along the confluence of the Chingshui River and the Chilukeng River [34] (the star mark at **Figures 3A** and **5A**).

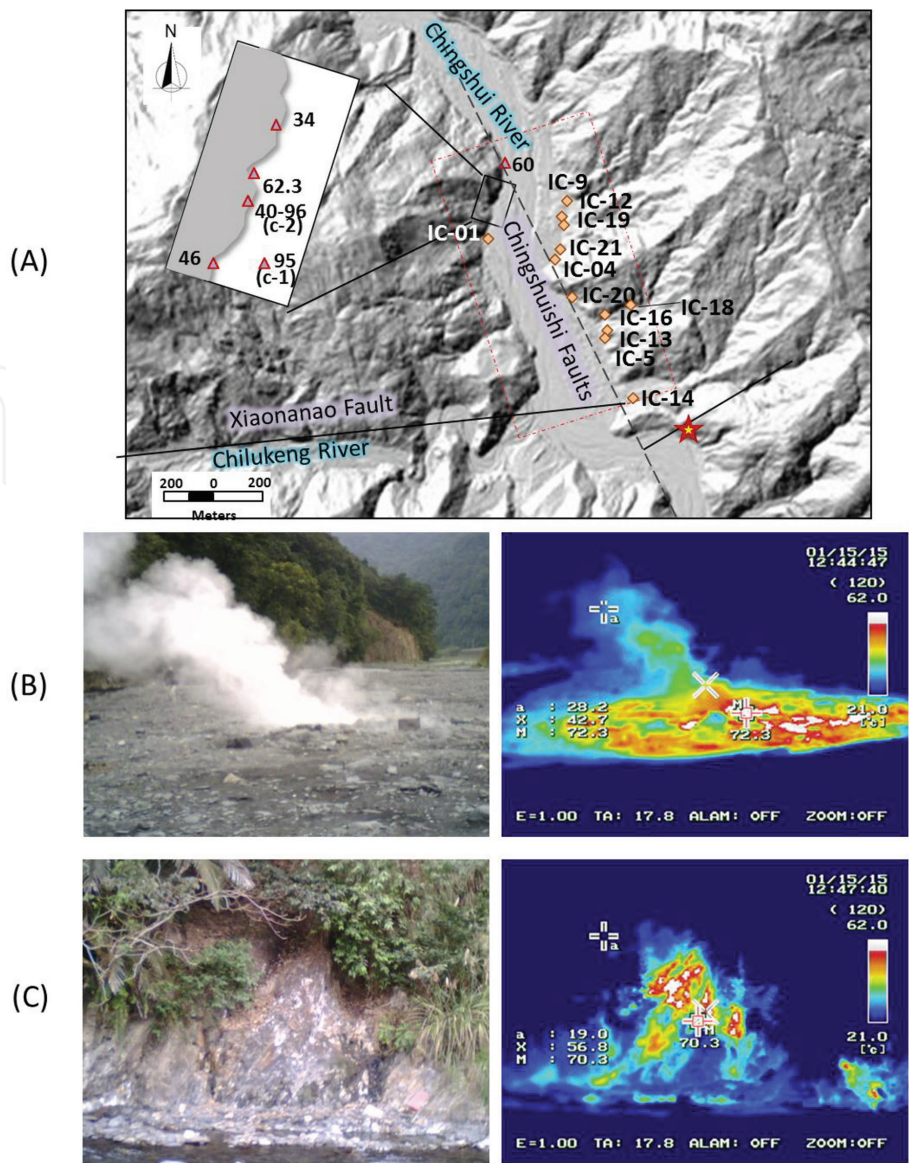


Figure 3.
(A) Distribution of surface temperature on rocks along the Chingshui River. (B) Thermal (left) and optical (right) images of hot springs along the riverbed. (C) Thermal (left) and optical (right) images of hot springs and fumaroles along the rock outcrops.



Figure 4.
The Xiaonanao Fault is a thrust fault with wide damage zones that are rich in quartz veins with euhedral pyramidal crystals on the outcrops along the Chilukeng River.

The fault gouge strikes ranging from N55°E to N75°E and dips from 30°N to 80°N. The mineral assemblage for these white veins is predominantly composed of calcite with minor quartz (Figure 5B).

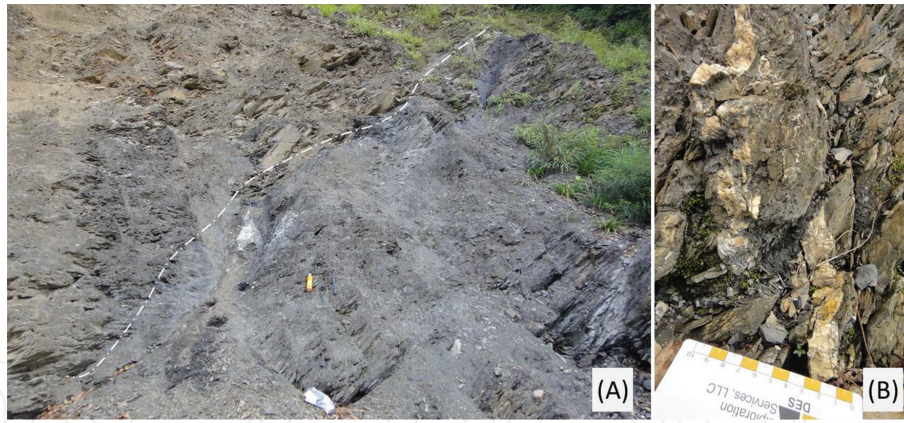


Figure 5. (A) A normal fault (white line), located at the confluence of Chingshui River and Chilukeng River (star mark at **Figure 3A**), is approximately 2 m wide with a steep dip and contains blocks of quartz veins. (B) The vein in the damage zone, cut by steep normal fault, is predominantly composed of calcite with minor quartz.

4. Geophysical explorations

Several geophysical exploration methods have been applied to the Chingshui geothermal field. They were geomagnetic, gravity, and resistivity surveys including transient electromagnetic (TEM), magnetotelluric (MT), and microseismicity.

4.1 Geomagnetic survey

Magnetic surveys record the spatial variation in the Earth's magnetic field, which the magnetic properties of rocks are measured. Generally, magnetic susceptibility is summarized as the various amounts of minor accessory minerals in all rocks, which contain iron-rich phases such as magnetite, pyrrhotite, and hematite. Magnetite is the most important magnetic mineral, because it is not only very common but also has relatively high magnetic susceptibility. A geomagnetic survey measures the changes in the amounts of magnetic minerals as well as associated rock types. A magnetic map, thus, helps locate mineral deposits by identifying specific rock types and geological features [35].

A total of 425 stations for geomagnetic survey in the Ilan Plain were performed in 1978 by Yu and Tsai [31]. They found an obvious WE high magnetic anomaly which is located between Ilan and Luodong, and they interpreted that this anomaly could be the magma intrusion as dikes underneath the Ilan area. Meanwhile, a low-magnetic zone between Chingshui and Hanhsi was observed by Tong et al. [30], which reprocessed the old data and elucidated that it might be associated with the destruction of magnetite in the host rocks by hydrothermal alteration. The fluid for hydrothermal alteration in the Chingshui area was probably related to the magmatic source also supported by oxygen and carbon isotopes [34].

4.2 Gravity survey

The purpose of gravity survey is to detect mass materials underneath the places, which are not uniformly the same everywhere. They vary with the distributions of the dense materials below. A gravity survey is an indirect method to get the density property of subsurface materials. The higher the gravity values, the denser the rock, such as igneous body beneath.

A gravity survey with a total of 636 stations in the Chingshui geothermal field was completed by the ITRI in 1976 [36]. Although the variation in gravity is not significant due to the fact that the rock formation in survey area is predominantly

composed of slates, the gravity on both sides of the Chingshui stream is apparently different [30], which may be related to fault cut through along the river. Euler deconvolution is a useful tool to interpret the gravity data rapidly and delineate structural contacts and depth estimation quickly [37, 38]. Based on the results of Euler deconvolution and known adjacent geological structures, several faults have been identified. They are the Xiaonanao, Chingshuihsi, and Kulu faults, which correspond with known faults introduced by Tseng [28] and Lin and Yang [33]. Meanwhile, three unknown faults, namely, the A-fault, B-fault, and C-fault, have also been recognized, which might be associated with the Niutou Fault with a SW–NE trend. The Chingshuihsi Fault was offset by the Xiaonanao Fault and the C-fault in the south and north of Chingshui, respectively, and the known geothermal field in this region is bounded by the C-fault and the Xiaonanao Fault [30, 33].

4.3 Resistivity surveys

Surface resistivity survey measures the electrical potentials in the ground around a current-carrying electrode depending on the electrical resistivity and distribution of the surrounding sediments and rocks. It applies an electrical current between two electrodes implanted in the ground to measure the difference of potential between two additional electrodes that do not carry current. The distribution of potential can be related theoretically to ground resistivity and their distributions for rock bodies, which are distributed in a horizontally stratified ground and the homogeneous masses separated by vertical planes [39]. Mineral grains in sediments and rocks are essentially nonconductive; except in some ores or metallic minerals, the resistivity of sediments and rocks is governed primarily by the amount of pore water, its resistivity, and the orientations of the pores. The differences of lithology have different resistivity, so the surveys can be used to detect bodies of anomalous materials or in estimating the depths of bedrocks [39]. Generally, since the resistivity of rocks is controlled primarily by the pore water conditions in a rock, the values cannot be directly interpreted in terms of lithology. However, zones of distinctive resistivity are associated with specific rock units on the basis of local field or drill hole information, and the surveys were used profitably to extend field investigations into areas with very limited or nonexistent data. Meanwhile, the resistivity surveys may be used as a reconnaissance method, to detect anomalies that can be further investigated by complementary geophysical methods and/or drill holes [39].

The ITRI conducted surface resistivity surveys, including the transient electromagnetic (TEM, the collinear and orthogonal dipole–dipole measurements) and magnetotelluric (MT) in the Chingshui area since the 1970s [30, 32, 40, 41]. They deployed both the transmitter and receiver dipole lengths at different distances, that is, 300–1300 m, separately for TEM. Four groups of apparent resistivity data sets were collected with four individual transmitter locations and were reprocessed and inverted with modern 2D and 3D inversion codes later [42, 43]. The inverted bipole-bipole results show the regional geological structures of the Chingshui area and reveal three vertical conductive structures, H, I, and J. They may correspond to the vertical Chingshuichi Fault, the stratigraphic boundary between the Chingshuihu member and Jentse member, and coincide to the Dachi Fault [28] and the Xiaonanao Fault, respectively [43]. Hot springs crops out along the Chingshuichi Fault, suggesting that it might be the conduit to provide geothermal fluids.

The magnetotelluric (MT) survey is a method to use frequently and successfully for exploring geothermal reservoirs [44–46]. Many reports claim that geothermal fluid circulates along the fractures within the meta-sandstones or slates in the Chingshui geothermal field [27, 28]. To detect the geological structures

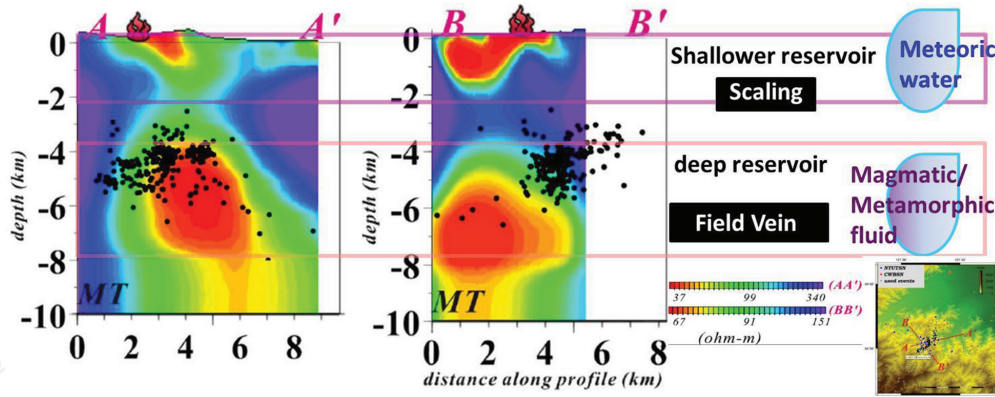


Figure 6.
Two-reservoir model with MT images and many microseismicity in the Chingshui geothermal field.

and reservoir underneath the Chingshui area, 33 broadband magnetotelluric data points were acquired by the ITRI in June 2006 [30]. Those data were processed and inverted for 1D and 2D images [30]. Moreover, the MT time series data were measured over 72 h at all stations to improve the data quality in 2014 and were processed using statistically robust algorithms from Jones et al. [47] for the MT 3D inversion [48].

The MT results could be achieved based on the understanding of the resistivity of various types of rocks in the survey area (**Figure 6**). A significant low-resistivity zone can be identified, which could be related to a clay-rich cap rock in the geothermal structure. The cap rock is about 1 km in width and is found at depths ranging between 200 and 1000 m [30]. The resistivity of the cap rock is about 14 Ωm [30], which is not as low as many other volcanic geothermal fields that have a low-resistivity cap layer of less than 5 Ωm . It is characterized by the Chingshui geothermal field having slate host rocks that are expected to be less reactive than the volcanic rocks. The cap rocks could be illite-rich slates, which got approved by recent drilling results [8].

The reservoir of Chingshui geothermal field is a typical fault-controlled fractures, which may be created by the several faults distributed in this area [30]. MT images show that the fractures associated with the geothermal reservoir are distributed from near surface to a depth of 1500 m toward the south in fault zones, which is similar to the identified production zone from the core drilling records. The size of the Chingshui geothermal reservoir is estimated to be about $9.54 \times 10^7 \text{ m}^3$ and contains about 10 million cubic meters of geothermal fluids, based on the 3D model with a gross porosity of 0.1 and 100% saturation for the fracture zones [42]. Meanwhile, two geothermal reservoirs have been proposed underneath the Chingshui geothermal field according to MT images (**Figure 6**) [8, 34, 48]. One is shallower at a depth of less than 3000 m, while the other is deeper at depths ranging from 4000 to 8000 m. Moreover, abundant microseismicity occurred at the top of the deep reservoir [49]. This result leads us to infer that the deep reservoir may be a high-temperature hydrothermal system with frequent hydraulic fracturing occurring that induces microseismicity.

5. Geochemical explorations

Geothermal exploration provides abundant information for the location, nature, and origin of the geothermal waters in a geothermal system. Geochemical studies of geothermal fluids involve three main steps: (1) sample collection, (2) chemical analysis, and (3) data interpretation [50]. The results give the parameters that are

sensitive to subsurface temperatures, salinity of the fluids, and gaseous chemical compositions in interesting areas. Meanwhile, the constituents of fluid chemistry are used to trace the origin and flow of geothermal waters, especially the stable isotopes, such as ^2H and ^{18}O , along with B and Cl being most important. Chemical constituents of rocks, for example, SiO_2 , Na, K, Ca, Mg, and CO_2 , are useful for estimating subsurface temperatures and potential production problems such as scaling and corrosion [50].

5.1 Geochemistry of fluids

Several hot springs cropped out on the surface, and 21 exploring and production wells have been drilled in the Chingshui geothermal field (**Figure 3A**). The temperatures and pH of springs and wells range from 48 to 99°C and 6.4 to 9.7 and from 180 to 230°C and 6.3 to 8.9, respectively [7]. The major gases of geothermal steam being about 20% in the Chingshui area are CO_2 , H_2S , and others. Carbon dioxide is generally the major gas component often comprising more than 97% of all non-condensable gases, and its concentration increases with reservoir temperature. Hydrogen sulfide concentration is about 1% and commonly decreases as steam ascends to the surface due to reaction with wall rock, dissociation to sulfur, or oxidation to SO_4 [7].

The chemical and isotopic compositions of hot spring and wells are shown in **Figures 7 and 8**. Chemical compositions of cations and anions in the Chingshui geothermal fluids are pretty variable. Bicarbonate ($[\text{HCO}_3^-] = 500\text{--}3200$ ppm) is the major anion in most geothermal waters, being with lower chloride ($[\text{Cl}^-] = 6.5\text{--}23.4$ ppm) and sulfate ($[\text{SO}_4^{2-}] = 29\text{--}72$ ppm), which are the bicarbonate fluid type based on Piper diagram (**Figure 7**) [51]. Sodium ($[\text{Na}^+] = 35\text{--}1235$ ppm) is the major cation in most geothermal fluids, being with lower calcium and magnesium (both few ppm). Based on the Na-K-Ca geothermometer, the temperatures of thermal fluids in reservoirs range from 137 to 205°C. Silica (SiO_2) compositions of thermal fluids range from 83 to 413 ppm, which are correlated to the temperature from 127 to 214°C, respectively, by silica geothermometry [7]. However, the SiO_2 geothermometer is a more reasonable and suitable method than Na-K-Ca one for assessing reservoir fluid temperatures in the slate region in Taiwan in terms of experimental fluid–rock interactions on laboratory [52, 53].

Hydrogen and oxygen isotopic compositions for meteoric water along LangyongSi River (the mainstream of Chingshui River) were $-70\text{~}+10\text{‰}$ and -11 to 0‰ , which may be due to rapid topographic change and strong monsoon effect in winter [54] (**Figure 8**). For the hot springs and thermal water, the δD and $\delta^{18}\text{O}$ values are $-67\text{~}-32\text{‰}$ and -9.2 to -4.4‰ and $-57\text{~}-24\text{‰}$ and -6.7 to -4.0‰ , respectively. The wide ranges of isotopic compositions in hot springs may be partly attributed to wider geographic distributions of them and mixing of thermal water with meteoric water [54]. Plots of H^- and O^- isotopic compositions of thermal water on the local meteoric water line (MWL) show the close relationship with the meteoric water (**Figure 8**). Isotopic changes of geothermal water due to fluid–rock interaction were small with a maximum $\delta^{18}\text{O}$ shift of about 3‰ from the MWL. This small shift may reflect the slow fluid–rock interaction in terms of low permeability of the slate host rocks [54].

5.2 Isotopes of carbonate veins and scaling

The hot fluids in Chingshui geothermal field are characteristic of high concentration of HCO_3^- . When the geothermal reservoir is breached by tectonic activities or drilling for geothermal exploitation, CO_2 is oversaturated and can be released

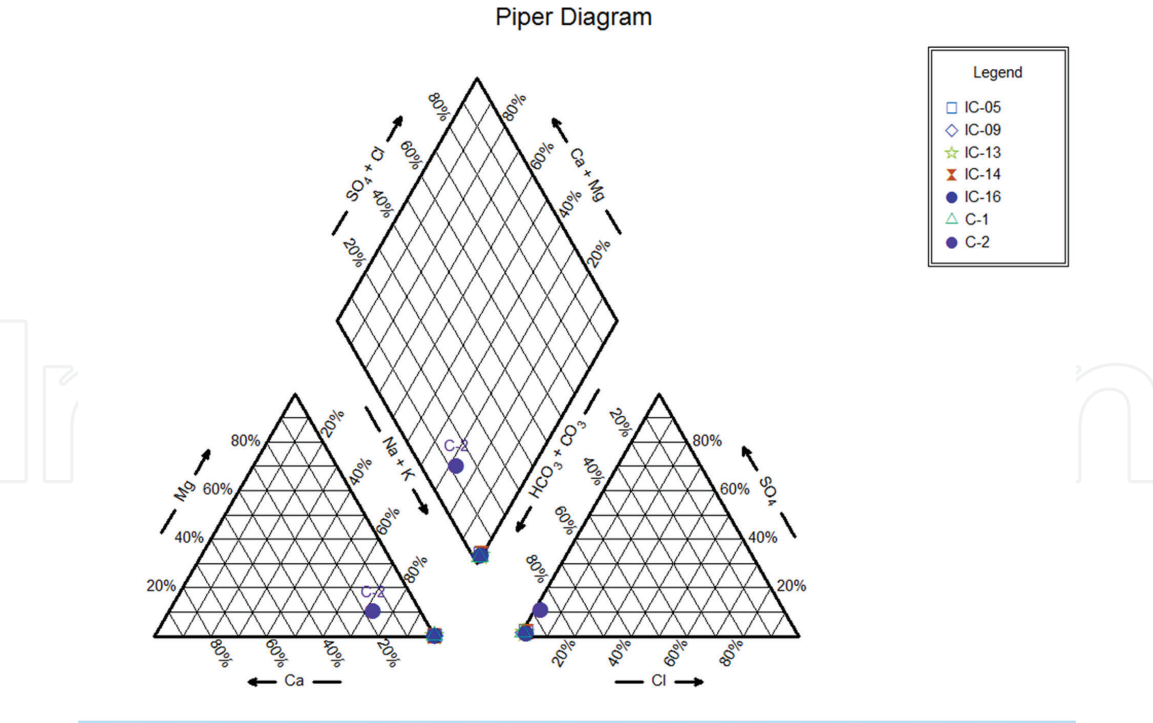


Figure 7. The water compositions of Chingshui area are plotted on the Piper diagram showing the typical Na-bicarbonate fluid type.

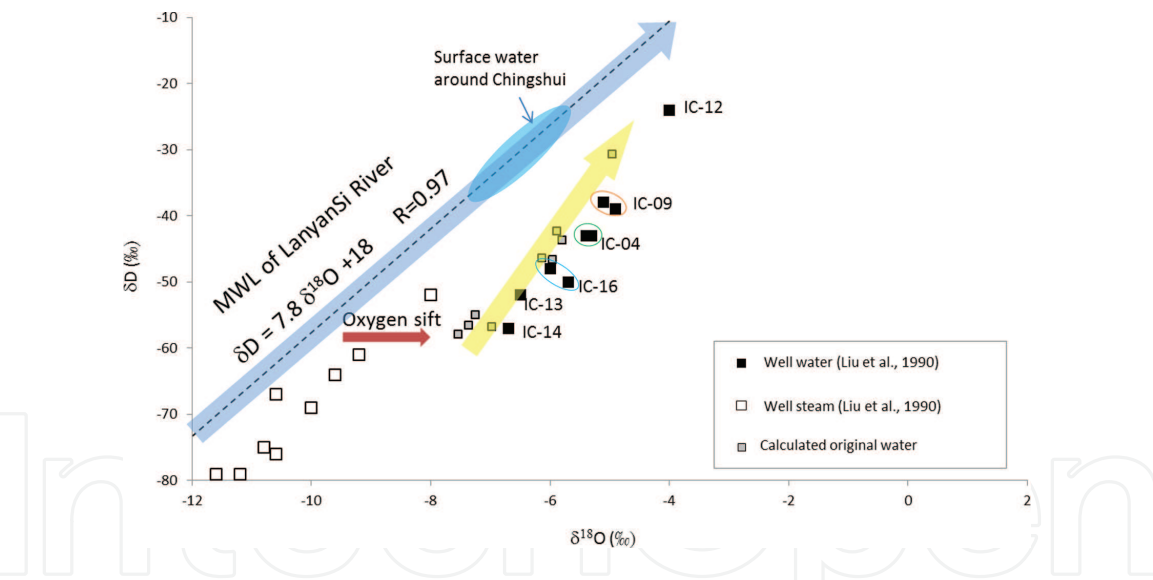


Figure 8. Plots of H- and O- isotopic compositions of thermal water on the local meteoric water line (MWL) show the close relationship with the meteoric water.

quickly by depressurization causing the bicarbonate solution to oversaturate rapidly with pH increase and to precipitate carbonate minerals from thermal water immediately. The isotopic data from fracture-filling carbonate minerals have been found to be particularly useful to constrain the geochemical characteristics of fluid reservoirs and possible post-depositional and syntectonic fluid processes [55–59].

Two populations of $\delta^{18}\text{O}$ values were recognized, $-5.8 \pm 0.8\text{‰}$ VSMOW from scaling in the wells and $-1.0 \pm 1.6\text{‰}$ to $10.0 \pm 1.3\text{‰}$ VSMOW from the calcite veins of outcrops (**Figure 9**), which are indicative of meteoric and magmatic fluid sources, respectively [34]. Meanwhile, two hydrothermal reservoirs at different depths have been identified by magnetotelluric (MT) imaging with microseismicity underneath this area [48, 49] (**Figure 6**). Two-reservoir model has been proposed: One is the

shallow reservoir with fluids from meteoric water to provide the thermal water for scaling depositions inside the production wells, while the deep one supplies magmatic fluids mixing with deep marble decarbonization to precipitate the calcite veins near fault zones [34]. Helium isotope data from Cheng [60] also provided strong evidence of magmatic fluids from the deeper reservoir in the Chingshui geothermal field. The ratios of $^3\text{He}/^4\text{He}$ were 3.8–4.0 RA and 0.8 RA for the samples. These lines of evidence indicated the existence of a mantle-derived component in the Chingshui area, which may be derived from magmatic degassing; however, the lower helium isotope ratio of the other sample also implied a mixing between such a deeper, magmatic-related reservoir and a shallower, crustal-related one [34, 60].

The well IC-21 commenced drilling at May 2010. Upper 600 m was drilled into the hole and did not take any cores, just a cutting per 10 m. Whole coring raised 200 m in length between 600 and 800 m in depth and got over 95% core recovery. Lithologically, the 200 m cores are predominantly composed of dark-gray to black slates occasionally intercalated with argillites or meta-sandstones. There are many deformation structures, fractured systems, and veins in the cores (**Figure 10**). It is characteristic that many scaling minerals are irregularly filled up in the fractures, veins, and open cracks.

Three types of calcite crystal morphologies have been identified in the veins of the cores: bladed, rhombic, and massive crystals (**Figure 11**). Bladed calcites are generated via degassing under boiling conditions with a precipitation temperature of $\sim 165^\circ\text{C}$ and calculated $\delta^{18}\text{O}$ value of -6.8‰ to -10.2‰ VSMOW for the thermal water [61]. Rhombic calcites grow in low-concentration Ca^{2+} and CO_3^{2-} [62–64] meteoric fluids and precipitate at approximately $\sim 180^\circ\text{C}$ [61]. Finally, massive calcites coprecipitated with quartz in the mixing zone of meteoric water and magmatic or metamorphic fluids with calculated $\delta^{18}\text{O}$ value of up to $1.5 \pm 0.7\text{‰}$ VSMOW. Furthermore, the scaling and hot fluids at a nearby pilot geothermal power plant confirm a meteoric origin. It indicates the current orientations of the main conduits for geothermal fluids are oriented at $\text{N}10^\circ\text{E}$ with a dip of 70°E [61].

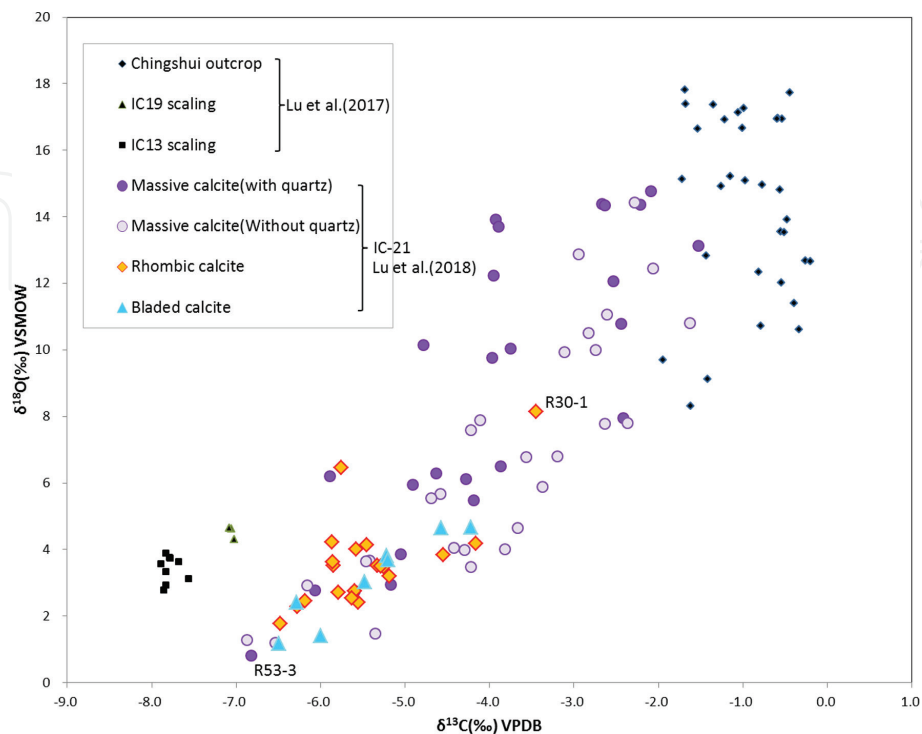


Figure 9.
Plots of carbon and oxygen isotope values of calcite veins and scaling from outcrops, IC-21, and wells in the Chingshui geothermal field.

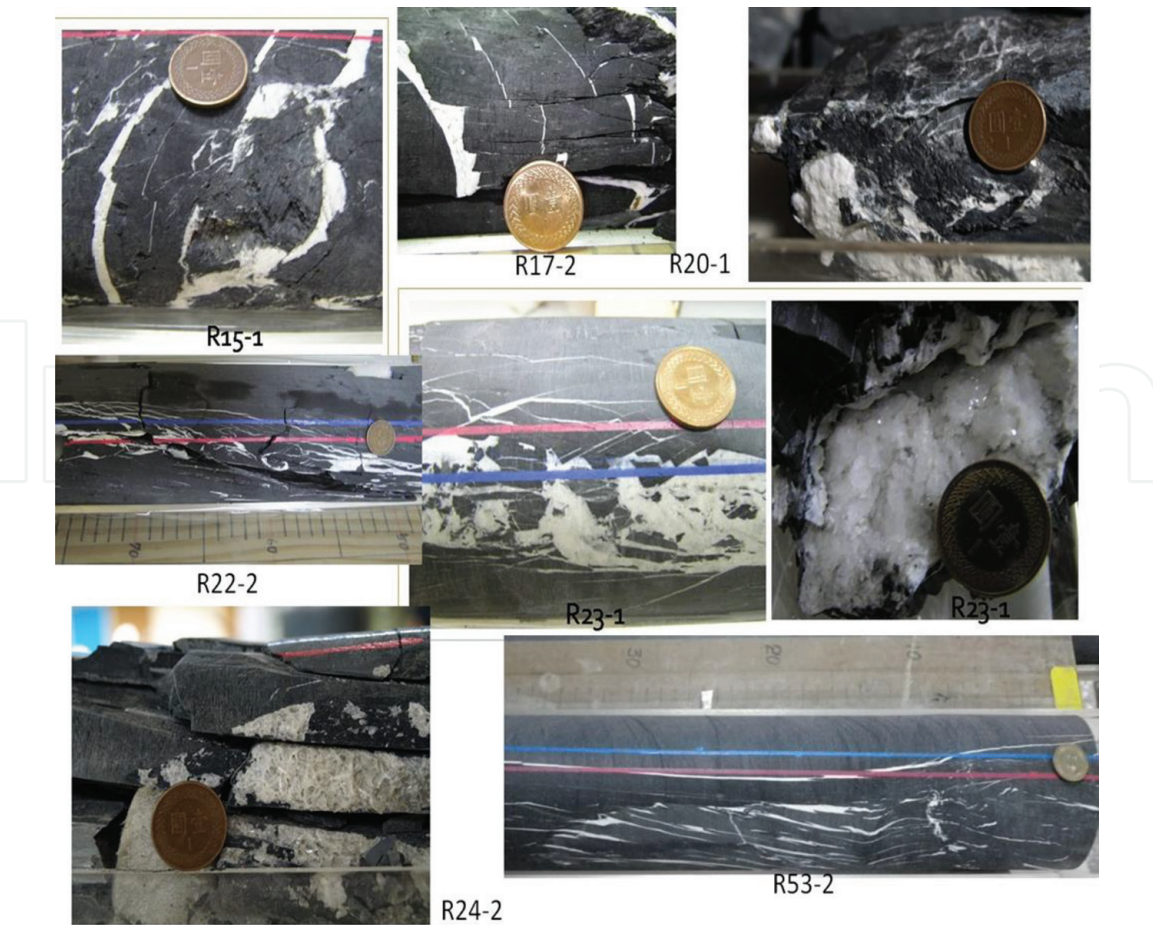


Figure 10.
Photos of veins in the core of well IC-21.

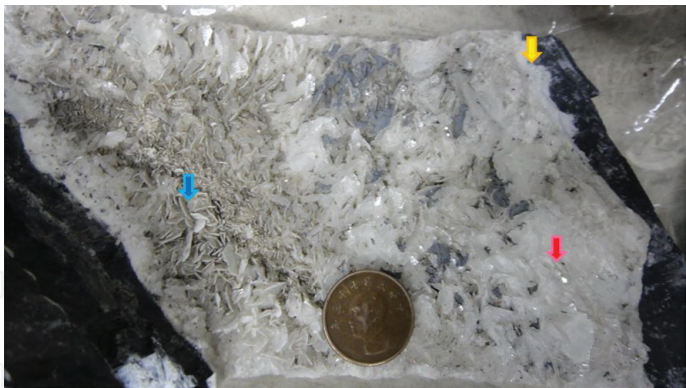


Figure 11.
Photographs of the calcite morphologies observed in the veins of IC-21 cores: massive (yellow arrow), rhombic (red arrow), and bladed calcites (blue arrow) in fractures. The diameter of 1 dollar coin is 2 cm for scales.

6. Conclusions

The Chingshui geothermal field, a moderate-temperature and water-dominated hydrothermal system, was the site of the first geothermal power plant in Taiwan. This article introduces the exploration results of a geothermal reservoir located in the slate formation of Taiwan using geological, geophysical, and geochemical methods. The hot springs, gas fumaroles with sulfur precipitation, hydrothermal alteration, and high surface temperature on rock body are the thermal manifestations in the Chingshui geothermal field. All of these manifestations are predominantly occurring in very narrow belt about 20–30 m

wide along the Chingshui River, which are controlled by the fractures of faults. Therefore, surface geological works provide abundant information on rock formations and fracture patterns to infer where and how deep the geothermal reservoir and probably current conduct circulation system are. Furthermore, to construct a model for understanding the subsurface rock bodies and geological structures.

Geophysical surveys including the geomagnetic, gravity, resistivity measurements (transient electromagnetic [TEM] and magnetotelluric [MT]), and micro-seismicity have been applied to detect the subsurface geological structures. A model with two geothermal reservoirs has been proposed underneath the Chingshui geothermal field. One is shallower at a depth of less than 3000 m, while the other is deeper at depths ranging from 4000 to 8000 m. Moreover, abundant micro-seismicity distributed at the top of the deep reservoir to infer a high-temperature hydrothermal system with frequent hydraulic fracturing occurred that induces microseismicity. However, the resolutions of geophysical surveys are not so high to precisely draw the whole picture of reservoirs and to pinpoint where the fault fractures as conduits for thermal fluid circulation due to the narrow of fault zones in the slate formation.

Chemical constituents of the Chingshui geothermal water are rich in bicarbonate and sodium in anion and cation, suggesting that it is the HCO_3^- - Na^+ fluid type based on Piper diagram. Based on the Na-K-Ca and silica geothermometers, the temperatures of thermal fluids in reservoirs range from 137 to 205°C and from 127 to 214°C, respectively. The H^- and O^- isotopic compositions of thermal water are close relationship with the meteoric water that indicate that the isotopic changes of geothermal water due to fluid-rock interaction were small. This small shift may reflect the slow fluid-rock interaction in terms of low permeability of the slate host rocks.

Carbon and oxygen isotopic analyses indicate that the samples from outcrops and scaling in geothermal wells possess the highest and lowest values, respectively. These results infer that the former could be derived from fluids originating from the shallower reservoir, while the latter may be from the deeper reservoir to precipitate calcite veins near the faults. The calculated oxygen isotopes of fluids combining with the ratios of $^3\text{He}/^4\text{He}$ suggest that the fluid in the deep may be from magmatic source underneath the Chingshui geothermal field, while the thermal water in shallower reservoir is a mixing between deep magmatic fluids with meteoric one. The original fluids of bladed calcites confirm a meteoric origin, which have the similar oxygen isotopic value with the thermal fluids of Chingshui. It indicates the current orientations of the main conduits for geothermal fluids are oriented at N10°E with a dip of 70°E.

Acknowledgements

This work was supported by the Ministry of Science and Technology (MOST), Taiwan, under the grants of NSC 102-3113-P-002-031, MOST 103-3113-M-002-001, MOST 104-3113-M-002-001, and MOST 105-3113-M-002-001.

IntechOpen

Author details


Sheng-Rong Song^{1*} and Yi-Chia Lu^{1,2}

1 Department of Geosciences, National Taiwan University, Taipei, Taiwan

2 Department of Earth Sciences, National Taiwan Normal University, Taipei, Taiwan

*Address all correspondence to: srsong@ntu.edu.tw

IntechOpen

© 2018 The Author(s). Licensee IntechOpen. This chapter is distributed under the terms of the Creative Commons Attribution License (<http://creativecommons.org/licenses/by/3.0>), which permits unrestricted use, distribution, and reproduction in any medium, provided the original work is properly cited. 

References

- [1] BOE. 2016. https://www.moeaboe.gov.tw/ECW/populace/content/ContentLink.aspx?menu_id=137&sub_menu_id=358 [WWW Document]. Bur. Energy, R.O.C
- [2] Taipower. No Title [WWW Document]; 2016
- [3] Ho CS. A synthesis of geologic evolution of Taiwan. *Tectonophysics*. 1986;**125**:1-16
- [4] Song SR, Yang TF, Yeh YH, Tsao S, Lo HJ. Tatun volcano group is active or extinct? *Journal of the Geological Society of China*. 2000;**43**:521-534
- [5] Moeck IS. Catalog of geothermal play types based on geologic controls. *Renewable and Sustainable Energy Reviews*. 2014;**37**:867-882. DOI: 10.1016/j.rser.2014.05.032
- [6] Song SR. The Geothermal Potentials and Opportunity in Taiwan. IGA-Asian Symposium Geothermal Energy. Offenburg, Germany; 2018
- [7] MRSO. Exploration of geothermal resources in Taiwan. Repub. China Rep 2. 1978. 75 p
- [8] Song SR. National Energy Program: The Study of Chingshui Geothermal Field (3/3). National Science Council 2012-Final Report (NSC 101-3113-M-002-001); 2012
- [9] Bertani R. Geothermal power generation in the world 2010-2014 update report. In: *Proceedings of World Geothermal Congress 2015*; Melbourne, Australia. 2015. pp. 1-19
- [10] Seno T, Maruyama S. Paleogeographic reconstruction and origin of the Philippine sea. *Tectonophysics*. 1984;**102**: 53-84
- [11] Tsai YB, Liaw ZS, Lee TQ, Lin MT, Yeh ZH. Seismological evidence of an active plate boundary in the Taiwan area. *Memoir of the Geological Society of China*. 1981;**4**:143-154
- [12] Yu SB, Chen HY. Global positioning system measurements of crystal deformation in the Taiwan arc-continent collision zone. *Terrestrial, Atmospheric and Oceanic Sciences*. 1994;**5**:477-498
- [13] Ching KE, Hsieh ML, Johnson KM, Chen KH, Rau RJ, Yang M. Modern vertical deformation rates and mountain building in Taiwan from precise leveling and continuous GPS observations, 2000-2008. *Journal of Geophysical Research*. 2011;**116**. DOI: 10.1029/2011JB008242
- [14] Teng LS. Geotectonic evolution of late Cenozoic arc-continent collision in Taiwan. *Tectonophysics*. 1990;**183**:57-76
- [15] Teng LS. Stratigraphic records of the late Cenozoic Penglai orogeny of Taiwan. *Acta Geologica Taiwanica*. 1987;**25**:205-224
- [16] Chen HF. Crustal uplift and subsidence in Taiwan: An account based upon retriangulation results. *Spec. Publ. Cent. Geol. Surv. Taiwan*. 1984;**3**:127-140
- [17] Peng TH, Li YH, Wu FT. Tectonic uplift rates of the Taiwan Island since the early Holocene. *Memoir of the Geological Society of China*. 1977;**2**:57-69
- [18] Yu SB, Chen HY, Kuo LC. Velocity field of GPS stations in the Taiwan area. *Tectonophysics*. 1997;**274**:41-59
- [19] Yu SB, Kuo LC, Punongbayan RS, Ramos EG. GPS observation of crustal deformation in the Taiwan-Luzon

- region. *Geophysical Research Letters*. 1999;**26**:923-926
- [20] Furukawa M, Tokuyama H, Abe S, Nishizawa A, Kinoshita H. Report on DELP 1988 cruises in the Okinawa trough, 2, Seismic reflection studies in the southwestern part of the Okinawa trough. *Earthquake Research Institute, University of Tokyo*. 1991; **66**:17-36
- [21] Kimura M. Back-arc rifting in the Okinawa trough. *Marine and Petroleum Geology*. 1985;**2**:222-240. DOI: 10.1016/0264-8172(85)90012-1
- [22] Sibuet JC, Deffontaines B, Hsu SK, Thureau N, Formal TPL, Liu CS, et al. Okinawa trough backarc basin: Early tectonic and magmatic evolution. *Journal of Geophysical Research*. 1998;**103**:245-267. DOI: 10.1029/98JB01823
- [23] Chen YG, Wu WS, Chen CH, Liu TK. A date for volcanic eruption inferred from a siltstone xenolith. *Quaternary Science Reviews*. 2001;**20**:869-873
- [24] Chang LS. Some planktonic foraminifera from the Suo and Urai Groups of Taiwan and their stratigraphical significance. *Proceedings of the Geological Society of China*. 1962;**5**:127-133
- [25] Chang LS. Tertiary planktonic foraminiferal zones of Taiwan and overseas correlation. *Memoir of the Geological Society of China*. 1962;**1**:107-112
- [26] Chen WS. An introduction to the geology of Taiwan explanatory text of the geologic map of Taiwan (1/400000). Taipei: Geological Society; 2016
- [27] Hsiao PT, Chiang SC. Geology and geothermal system of the Chingshui-Tuchang geothermal area, Ilan, Taiwan. *Petroleum Geology of Taiwan*. 1979;**16**:205-213
- [28] Tseng CS. Geology and geothermal occurrence of the Chingshui and Tuchang Districts, Ilan. *Petroleum Geology of Taiwan*. 1978;**15**:11-23
- [29] Lin CW, Lin WH. Explanatory text of the geologic map of Taiwan Sanshin. Sheet 15. Taiwan: Cent. Geol. Surv. MOEA; 1995
- [30] Tong LT, Ouyang S, Guo TR, Lee CR, Hu KH, Lee CL. Insight into the geothermal structure in Chingshui, Ilan, Taiwan. *Terrestrial, Atmospheric and Oceanic Sciences*. 2008;**19**:413-424. DOI: 10.3319/TAO.2008.19.4.000
- [31] Yu SB, Tsai YB. Geomagnetic anomalies of the Ilan plain, Taiwan. *Petroleum Geology of Taiwan*. 1979;**16**:19-27
- [32] Su F. Resistivity survey in the Chingshui prospect, I-Lan, Taiwan. *Petroleum Geology of Taiwan*. 1978;**15**:255-264
- [33] Lin CW, Yang CN. Structure styles of the slate and schist belts in northeastern Taiwan. *Bulletin of the Geological Survey of Japan*. 1999;**12**
- [34] Lu YC, Song SR, Wang PL, Wu CC, Mii HS, MacDonald J, et al. Magmatic-like fluid source of the Chingshui geothermal field, NE Taiwan evidenced by carbonate clumped-isotope paleothermometry. *Journal of Asian Earth Sciences*. 2017;**149**:124-133. DOI: 10.1016/j.jseaes.2017.03.004
- [35] Stevenson DJ. Planetary magnetic fields: Achievements and prospects. *Space Science Reviews*. 2010;**152**:651-664. DOI: 10.1007/s11214-009-9572-z
- [36] Lee CR. Compilation of the geothermal prospects data in Taiwan during 1966-1979. *Bur. Energy Rep 500*; 1994

- [37] Keating PB. Weighted Euler deconvolution of gravity data. *Geophysics*. 1998;**63**:1595-1603
- [38] Roy L, Agarwal BNP, Shaw RK. A new concept in Euler deconvolution of isolated gravity anomalies. *Geophysical Prospecting*. 2000;**48**:559-575
- [39] Wightman WE, Jalinoos F, Sirles P, Hanna K. Application of Geophysical Methods to Highway Related Problems. Publication No. FHWA-IF-04-021. Lakewood, CO: Federal Highway Administration, Central Federal Lands Highway Division; 2003
- [40] Cheng WT, Lee FC. Bipole-dipole resistivity mapping in the Chingshui geothermal area. *Mining and Metallurgy*. 1977;**21**:88-93
- [41] Chiang SC a, Liu YF. Application of TDEM method in the Chingshui geothermal area, Ilan, Taiwan. *Petroleum Geology of Taiwan*. 1983;**19**:197-218
- [42] Chang PY, Lo W, Song SR, Ho KR, Wu CS, Chen CS, et al. Evaluating the Chingshui geothermal reservoir in northeast Taiwan with a 3D integrated geophysical visualization model. *Geothermics*. 2014;**50**:91-100. DOI: 10.1016/j.geothermics.2013.09.014
- [43] Ho G, Chang P, Lo W, Liu C, Song S. New evidence of regional geological structures inferred from reprocessing and resistivity data interpretation in the Chingshui-Sanshing-Hanchi area of southwestern Ilan County, NE Taiwan. *Terrestrial Atmospheric and Oceanic Sciences*. 2014;**25**:491-504. DOI: 10.3319/TAO.2014.01.24.01(TT)1
- [44] Uchida T, Song Y, Lee TJ, Mitsuhata Y, Lim SKL, Lee SK. Magnetotelluric survey in an extremely noisy environment at the Pohang low-enthalpy geothermal area, Korea. In: *Proceedings of World Geothermal Congress*. Turkey; 2005
- [45] Ushijima K, Mustopa EJ, Jotaki H, Mizunaga H. Magnetotelluric soundings in the Takigami geothermal area, Japan. In: *World Geothermal Congress*. 24-29; 2005
- [46] Wannamaker PE, Rose PE, Doerner WM, Berard BC, McCulloch J, Nurse K. Magnetotelluric surveying and monitoring at the coso geothermal area, California, in support of the enhanced geothermal systems concept: Survey parameters and initial results. In: *Proc. World Geotherm. Congr.* 2005; April 2005 24-29; Antalya, Turkey. 2004. pp. 24-29
- [47] Jones AG, Chave AD, Egbert G, Auld D, Bahr K. A comparison of techniques for magnetotelluric response function estimation. *Journal of Geophysical Research - Solid Earth*. 1989;**94**:14201-14213. DOI: 10.1029/JB094iB10p14201
- [48] Chiang CW, Hsu HL, Chen CC. An investigation of the 3D electrical resistivity structure in the Chingshui Geothermal area, NE Taiwan. *Terrestrial, Atmospheric and Oceanic Sciences*. 2014;**26**:269-281. DOI: 10.3319/TAO.2014.12.09.01(T)
- [49] Liu HF. Study of microseismicity and traveltime tomography in the Chingshui geothermal area [master's thesis]. National Taiwan University; 2013
- [50] Mwangi SM. Application of geochemical methods in geothermal exploration in Kenya. *Procedia Earth and Planetary Science*. 2013;**7**:602-606
- [51] Piper AM. A graphic procedure in the geo-chemical interpretation of water analysis. *Transactions of the American Geophysical Union*. 1953;**25**:914-928. DOI: 10.1029/TR025i006p00914
- [52] Huang JS, Peng DH. Subsurface geological report of IC-4 well

Ching-Shui, I-Lan, Taiwan. *Pet. Explor. Div.* 1976:1-13

[53] Huang YH, Liu HL, Song SR, Chen HF. An ideal geothermometer in slate formation: A case from the Chingshui geothermal field, Taiwan. *Geothermics*. 2018;**74**:319-326. DOI: 10.1016/j.geothermics.2017.11.002

[54] Liu KK, Yui TF, Shieh YN, Chiang SC, Chen LH, Hu JY. Hydrogen and oxygen isotope compositions of meteoric and thermal waters from the Chingshui geothermal area, northeastern Taiwan. *Proceedings of the Geological Society of China*. 1990;**33**:143-165

[55] Iwatsuki T, Satake H, Metcalfe R, Yoshida H, Hama K. Isotopic and morphological features of fracture calcite from granitic rocks of the Tono area, Japan: A promising palaeohydrogeological tool. *Applied Geochemistry*. 2002;**17**:1241-1257. DOI: 10.1016/S0883-2927(01)00129-9

[56] Li R, Dong S, Lehrmann D, Duan L. Tectonically driven organic fluid migration in the Dabashan Foreland Belt: Evidenced by geochemistry and geothermometry of vein-filling fibrous calcite with organic inclusions. *Journal of Asian Earth Sciences*. 2013;**75**: 202-212. DOI: 10.1016/j.jseas. 2013.07.026

[57] Luetkemeyer PB, Kirschner D, Huntington KW, Chester JS, Chester FM, Evans JP. Constraints on paleofluid sources using the clumped-isotope thermometry of carbonate veins from the SAFOD (San Andreas Fault Observatory at Depth) borehole. *Tectonophysics*. 2016. DOI: 10.1016/j.tecto.2016.05.024

[58] Wallin B, Peterman Z. Calcite fracture® fillings as indicators of paleohydrology at Laxemar at the Aspo Hard Rock Laboratory; southern Sweden. *Applied Geochemistry*. 1999;**14**

[59] Wang PL, Wu JJ, Yeh EC, Song SR, Chen YG, Lin LH. Isotopic constraints of vein carbonates on fluid sources and processes associated with the ongoing brittle deformation within the accretionary wedge of Taiwan. *Terra Nova*. 2010;**22**:251-256. DOI: 10.1111/j.1365-3121.2010.00940.x

[60] Cheng Y. Geochemical characteristics of groundwater in the Ilan Plain, Northeast Taiwan [master's thesis]. *Natl. Taiwan Univ.* 2014. pp. 1-82

[61] Lu YC, Song SR, Taguchi S, Wang PL, Yeh EC, Lin YJ, et al. Evolution of hot fluids in the Chingshui geothermal field inferred from crystal morphology and geochemical vein data. *Geothermics*. 2018;**74**:305-318. DOI: 10.1016/j.geothermics.2017.11.016

[62] Domingo C, Loste E, Garc J, Fraile J. Calcite precipitation by a high-pressure CO₂ carbonation route. *The Journal of Supercritical Fluids*. 2006;**36**:202-215. DOI: 10.1016/j.supflu.2005.06.006

[63] Lahann RW. A chemical model for calcite crystal growth and morphology control. *Journal of Sedimentary Research*. 1978;**48**:337-347

[64] Moore CH, Wade WJ. Carbonate diagenesis: Introduction and tools. In: *Carbonate Reservoirs*. Elsevier Inc; 2013. pp. 1-392